



HAL
open science

MAVEN observations of magnetic flux ropes with a strong field amplitude in the Martian magnetosheath during the ICME passage on 8 March 2015

Takuya Hara, Janet G. Luhmann, Jasper S. Halekas, Jared R. Espley, Kanako Seki, David A. Brain, Hiroshi Hasegawa, James P. Mcfadden, David L. Mitchell, Christian Mazelle, et al.

► To cite this version:

Takuya Hara, Janet G. Luhmann, Jasper S. Halekas, Jared R. Espley, Kanako Seki, et al.. MAVEN observations of magnetic flux ropes with a strong field amplitude in the Martian magnetosheath during the ICME passage on 8 March 2015. *Geophysical Research Letters*, 2016, 43, pp.4816-4824. 10.1002/2016GL068960 . insu-03670238

HAL Id: insu-03670238

<https://insu.hal.science/insu-03670238>

Submitted on 17 May 2022

HAL is a multi-disciplinary open access archive for the deposit and dissemination of scientific research documents, whether they are published or not. The documents may come from teaching and research institutions in France or abroad, or from public or private research centers.

L'archive ouverte pluridisciplinaire **HAL**, est destinée au dépôt et à la diffusion de documents scientifiques de niveau recherche, publiés ou non, émanant des établissements d'enseignement et de recherche français ou étrangers, des laboratoires publics ou privés.

Copyright

RESEARCH LETTER

10.1002/2016GL068960

Key Points:

- MAVEN detected strong field amplitude flux ropes in the magnetosheath during ICME passage in March 2015
- Such strong flux ropes (>80 nT) are first detected at the high altitudes (>5000 km) at Mars
- Estimated traveling velocity of flux ropes is at least an order of magnitude faster than usual cases

Supporting Information:

- Figure S1
- Supporting Information S1

Correspondence to:

T. Hara,
hara@ssl.berkeley.edu

Citation:

Hara, T., et al. (2016), MAVEN observations of magnetic flux ropes with a strong field amplitude in the Martian magnetosheath during the ICME passage on 8 March 2015, *Geophys. Res. Lett.*, 43, 4816–4824, doi:10.1002/2016GL068960.

Received 1 APR 2016

Accepted 5 MAY 2016

Accepted article online 13 MAY 2016

Published online 28 MAY 2016

MAVEN observations of magnetic flux ropes with a strong field amplitude in the Martian magnetosheath during the ICME passage on 8 March 2015

Takuya Hara¹, Janet G. Luhmann¹, Jasper S. Halekas², Jared R. Espley³, Kanako Seki⁴, David A. Brain⁵, Hiroshi Hasegawa⁶, James P. McFadden¹, David L. Mitchell¹, Christian Mazelle^{7,8}, Yuki Harada¹, Roberto Livi¹, Gina A. DiBraccio³, John E. P. Connerney³, Laila Andersson⁵, and Bruce M. Jakosky⁵

¹Space Sciences Laboratory, University of California, Berkeley, California, USA, ²Department of Physics and Astronomy, University of Iowa, Iowa City, Iowa, USA, ³NASA Goddard Space Flight Center, Greenbelt, Maryland, USA, ⁴Department of Earth and Planetary Science, Graduate School of Science, University of Tokyo, Tokyo, Japan, ⁵Laboratory for Atmospheric and Space Physics, University of Colorado Boulder, Boulder, Colorado, USA, ⁶Institute of Space and Astronautical Science, Japan Aerospace Exploration Agency, Sagami-hara, Japan, ⁷CNRS, Institut de Recherche en Astrophysique et Planétologie, Toulouse, France, ⁸IRAP, Université Paul Sabatier, Toulouse, France

Abstract We present initial results of strong field amplitude flux ropes observed by Mars Atmosphere and Volatile Evolution (MAVEN) mission around Mars during the interplanetary coronal mass ejection (ICME) passage on 8 March 2015. The observed durations were shorter than 5 s and the magnetic field magnitudes peaked above 80 nT, which is a few times stronger than those usually seen in the magnetosheath barrier. These are the first unique observations that MAVEN detected such flux ropes with a strong field at high altitudes (>5000 km). Across these structures, MAVEN coincidentally measured planetary heavy ions with energies higher than a few keV. The spatial properties inferred from the Grad-Shafranov equation suggest that the speed of the structure can be estimated at least an order of magnitude faster than those previously reported quiet-time counterparts. Hence, the space weather event like the ICME passage can be responsible for generating the observed strong field, fast-traveling flux ropes.

1. Introduction

The supersonic solar wind plasma directly interacts with the Martian upper atmosphere, because Mars lacks a global intrinsic magnetic field except for the crustal fields primarily localized in the southern hemisphere [e.g., Acuña *et al.*, 1998, 1999]. The plasma environment around Mars is thus susceptible to the solar wind, depending on upstream conditions/properties, such as the dynamic pressure and the interplanetary magnetic field (IMF) strength and orientation. Spacecraft measurements by Phobos 2 and Mars Express (MEX) have shown that the planetary ions are energized, resulting in their escape to interplanetary space [e.g., Lundin *et al.*, 1989; Barabash *et al.*, 2007; Lundin, 2011, and references therein]. The MEX plasma observations for more than a decade allow us to prove that global planetary ion escape rates positively correlate with the upstream dynamic pressure, EUV fluxes, as well as the solar activity proxies $F_{10.7}$, and the sunspot number [e.g., Lundin *et al.*, 2008; Nilsson *et al.*, 2010; Lundin *et al.*, 2013].

Mars Atmosphere and Volatile Evolution (MAVEN) mission has now been adding to these measurements around Mars since September 2014 [Jakosky *et al.*, 2015a, 2015b]. In order to especially investigate the Martian plasma environment and upper atmosphere, MAVEN possesses the most comprehensive set of instruments to measure particles (including ions, electrons, and neutral atoms) and electromagnetic fields so far in the Martian orbiter exploration history [Jakosky *et al.*, 2015a]. MAVEN also directly observes significant amounts of planetary heavy ions escaping into interplanetary space [e.g., Jakosky *et al.*, 2015b; Brain *et al.*, 2015]. The estimated present global ion escape rates affecting Mars are consistent with previous spacecraft measurements [e.g., Brain *et al.*, 2015; Y. Dong *et al.*, 2015].

The plasma environment around unmagnetized planets like Mars and Venus can be drastically changed during space weather events, including solar energetic particle events, and the disturbed solar wind structures including corotating interaction regions (CIRs), and interplanetary coronal mass ejections (ICMEs).

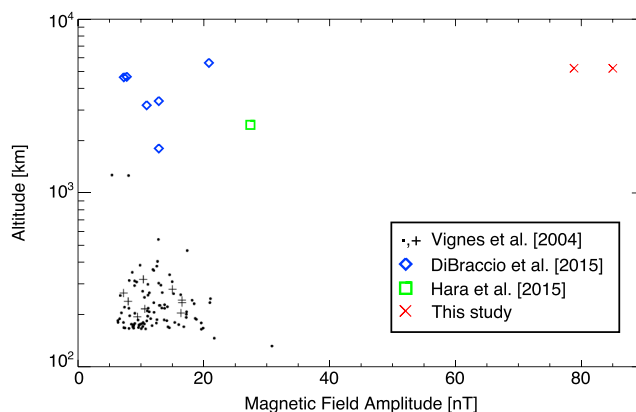


Figure 1. Flux rope magnetic field amplitude as a function of the observed altitude. The events observed by MGS around the subsolar (terminator) regions during the premapping phase are denoted as black pluses (filled circles) [Vignes *et al.*, 2004]. Blue diamonds and a green square were those observed by MAVEN [DiBraccio *et al.*, 2015; Hara *et al.*, 2015]. Red crosses are presented in this paper. Adapted to reproduce from Vignes *et al.* [2004].

A number of previous studies have discussed aspects of space weather effects on planets without a large-scale planetary magnetic field. Several authors reported that the global ion escape rates during space weather events can increase by a factor of between ~ 2 and 10 at least for both Mars and Venus, compared with the steady solar wind periods [e.g., Luhmann *et al.*, 2007, 2008; Futaana *et al.*, 2008; Dubinin *et al.*, 2009; Edberg *et al.*, 2010, 2011]. The plasma boundaries and ionospheric plasma around Mars can be compressed because of dynamic pressure increases driven by CIR and/or ICME passages [e.g., Opgenoorth *et al.*, 2013; Morgan *et al.*, 2014].

Recently, MAVEN recorded a couple of ICME structures passing Mars during early March 2015 [Jakosky *et al.*, 2015c]. In this paper, we present initial results of MAVEN measurements with respect to characteristic strong field amplitude magnetic flux ropes observed at quite high altitudes (>5000 km), as a new remarkable aspect of space weather effects seen in the Martian plasma environment. Magnetic flux ropes are characteristic twisted helical magnetic field structures [e.g., Russell and Elphic, 1979]. Figure 1 summarizes previous flux rope observations around Mars, distributed onto the observed flux ropes' field amplitude and altitude. Mars Global Surveyor (MGS) detected a lot of flux ropes mainly lower than 1000 km, which have a peak field of weaker than 20 nT and a radius of ~ 40 – 50 km [e.g., Cloutier *et al.*, 1999; Vignes *et al.*, 2004; Briggs *et al.*, 2011]. MAVEN also observes flux rope structures even higher than 1000 km in the Martian induced magnetosphere and magnetotail [Hara *et al.*, 2015; DiBraccio *et al.*, 2015]; however, their field amplitudes are typically smaller than 30 nT. Figure 1 clearly shows that the events, presented in detail later, are so unique observations at the high altitude (>5000 km) that their field amplitudes are a few times stronger than previous events. In this case associated with an ICME passage, the extreme properties of the structure and its possible consequences for enhanced ion escape merit special note. It should also be noticed that large-scale ($\gtrsim 100$ km) flux ropes with a peak field amplitude of stronger than 100 nT have also been detected often around strong crustal magnetic fields (not plotted onto Figure 1) [e.g., Brain *et al.*, 2010; Morgan *et al.*, 2011; Beharrell and Wild, 2012; Hara *et al.*, 2014a].

2. Overview of ICME Events Observed by MAVEN on March 2015

The upstream solar wind around Mars was quite disturbed on the beginning of March 2015, because a few ICMEs impacted Mars. Figure 2 represents the upstream solar wind conditions around Mars observed by the Solar Wind Ion Analyzer (SWIA) [Halekas *et al.*, 2015] and magnetometer (MAG) [Connerney *et al.*, 2015] experiments on board MAVEN for 10 days beginning on 1 March 2015. MAVEN observed three interplanetary shocks (vertical dashed green lines in Figure 2) associated with ICMEs. In particular, the 8 March event was the most extreme among them, because the solar wind velocity was greater than ~ 800 km/s, the corresponding dynamic pressure reached over 10 nPa, and the magnetic field amplitude also increased up to ~ 20 nT after the ICME shock. These disturbed solar wind parameters represent the most major overall external plasma and field disturbance during the MAVEN primary mission to date.

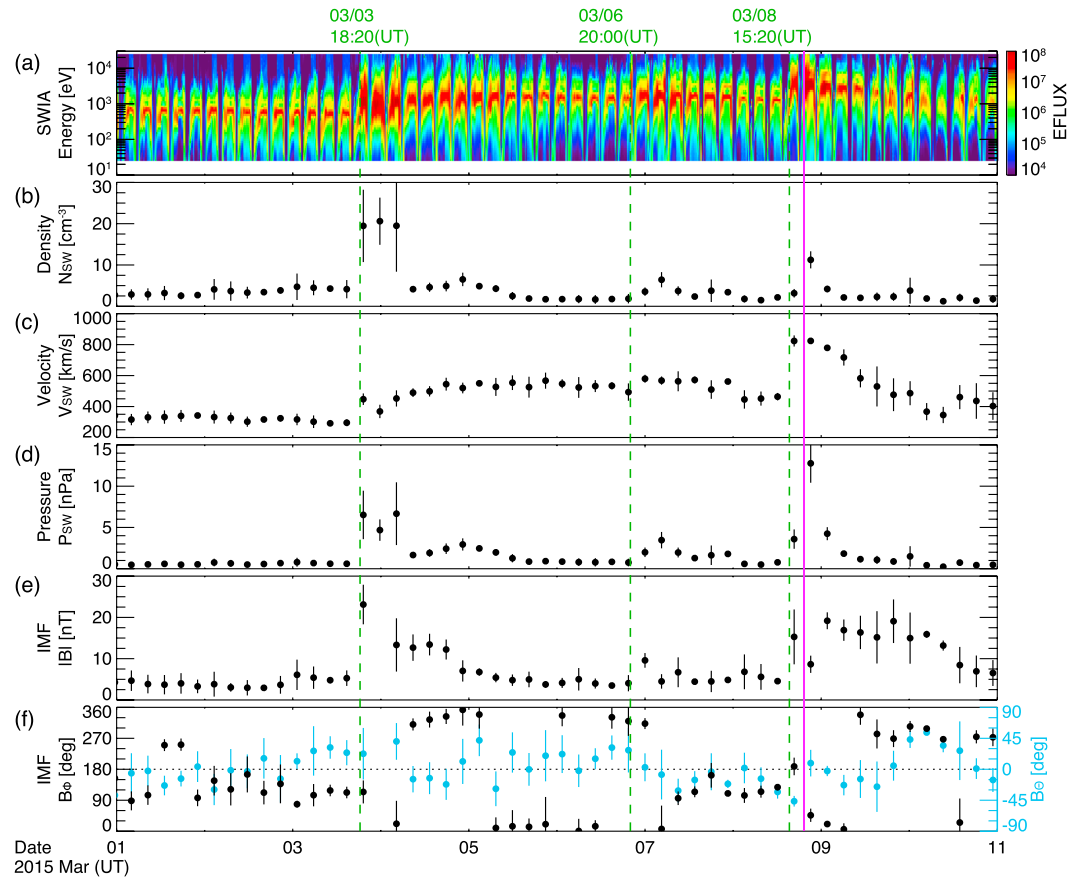


Figure 2. (a) SWIA omnidirectional energy time spectrogram in units of differential energy flux: $\text{eV}/\text{cm}^2/\text{s}/\text{str}/\text{eV}$, averaged over every 10 min, so that it can be easier to visually see the upstream dynamic variations. The other panels are an overview of the orbital mean upstream solar wind values (with the standard deviations shown as vertical lines) as derived from SWIA and MAG for 10 days from 1 March 2015: the solar wind (b) number density (N_{sw}), (c) velocity (V_{sw}), (d) dynamic pressure (P_{sw}), (e) IMF strength ($|\mathbf{B}|$), and IMF azimuth ($B_\phi \equiv \arctan(B_y/B_x)$; black) and elevation angles ($B_\theta \equiv \arcsin(B_z/|\mathbf{B}|)$; light blue) in the Mars-centered Solar Orbital (MSO) coordinates. The MSO coordinates are defined with the X_{mso} axis toward the Sun, the Z_{mso} axis perpendicular to the ecliptic pointing to the northern hemisphere, and the Y_{mso} axis completing the right-hand system. Figure 2a displays somewhat cyclic patterns, because MAVEN has an elliptical orbit capable of measuring various plasma regimes (e.g., upstream solar wind, magnetosheath, induced magnetosphere, and ionosphere), and its orbital period is about 4.5 h. The orbital mean solar wind is derived from simply averaging the SWIA and MAG data, when MAVEN was assumed to be in the solar wind region outside the empirical Martian bow shock [Trotignon *et al.*, 2006]. The three vertical green dashed lines are times when interplanetary shocks associated with ICMEs reached, inferred from discontinuity signatures (Figure 2a). Flux ropes presented here were observed in the magenta vertical line (see Figure 3 in detail).

Based on MAVEN comprehensive measurements, several aspects of the Martian plasma environment in response to the ICME passages are extensively described in Jakosky *et al.* [2015c]. For example, the inferred global escape rates of planetary heavy ions during these ICME events were substantially enhanced by about an order of magnitude over the usual rates, consistent with previous spacecraft measurements [e.g., Futaana *et al.*, 2008; Dubinin *et al.*, 2009; Edberg *et al.*, 2010]. Energetic planetary heavy ions picked up by the IMF embedded in the solar wind, often referred to as the “polar plume”, were accelerated by the convective electric field to energies more than 100 keV as the solar wind velocity rapidly increased within the space sampled by the MAVEN orbit. The multifluid MHD model during this event successfully reproduced the global features of the Martian plasma environment as observed by MAVEN [C. F. Dong *et al.*, 2015]. These models predict that the total ion escape rate was increased especially during the shock sheath phase just after the interplanetary shock arrival [C. F. Dong *et al.*, 2015; Curry *et al.*, 2015]. A kinetic test particle simulation suggests that planetary heavy ions precipitating back into the upper atmosphere were also highest during the shock sheath phase [Curry *et al.*, 2015]. The multifluid MHD simulation indicates that the ICME effects are not significant in the main Martian ionosphere (below 200 km) [C. F. Dong *et al.*, 2015]. However, these models do not include

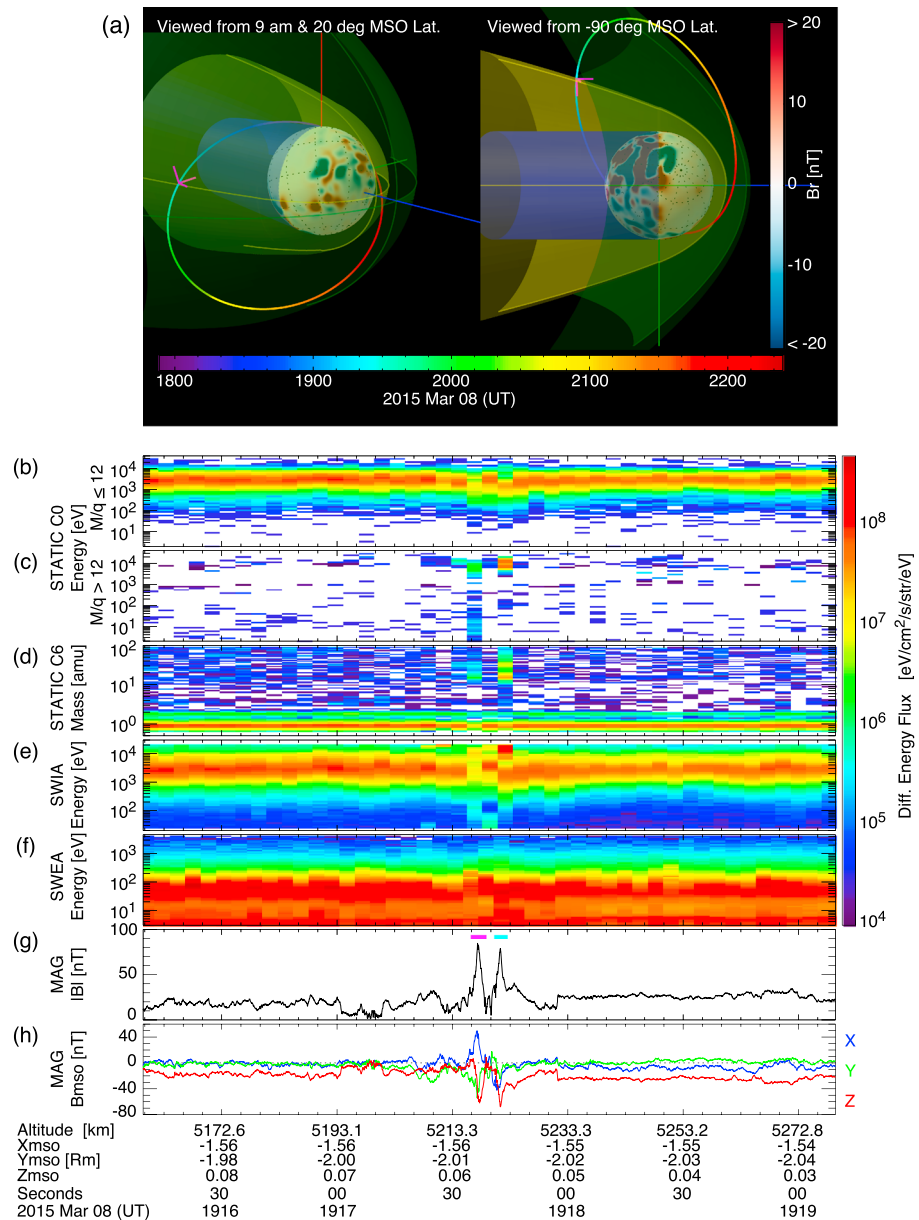


Figure 3. Overview of MAVEN observations for two magnetic flux ropes in the Martian magnetosheath during the ICME passage on 8 March 2015: (a) The MAVEN three-dimensional orbital configuration, viewed from (left) +20° MSO latitude at the 9:00 A.M. local time, and (right) −90° MSO latitude (i.e., $-Z_{mso}$ axis). The empirical bow shock and induced magnetosphere boundaries [Trotignon et al., 2006] are displayed as green and yellow surfaces. A blue surface is an optical shadow. The blue, green, and red bars represent the X_{mso} , Y_{mso} , and Z_{mso} axes, respectively. MAVEN orbited along the rainbow curve. Background blue-red color is a modeled radial component of the crustal field (B_r) at ~400 km altitude [Morschhauser et al., 2014], projected onto the globe surface, when MAVEN detected flux ropes. Flux ropes are observed at the magenta orthogonal three axes. The other panels are the zoomed-up plasma and magnetic field time series data across their structures: STATIC (b) light ($M/q \leq 12$) and (c) heavy ($M/q > 12$) ions omnidirectional energy, where M means the ion mass and q is the electric charge, (d) mass, (e) SWIA ion, and (f) SWEA electron omnidirectional energy spectra. Magnetic field (g) amplitude and (h) vector components in the MSO coordinate system measured by MAG. The magenta and light blue horizontal bars inside Figure 3g are events time segments.

the effects of particle precipitations related to these events. For example, the diffuse aurora emissions, likely caused by the related solar energetic electrons [Schneider *et al.*, 2015], most likely cause additional impact ionization, while the expected sputtering caused by the observed precipitating heavy ions could not be directly measured.

3. MAVEN Observations of Flux Ropes During ICME Passage

Figure 3 shows two magnetic flux rope events observed about 4 h after the 8 March ICME shock arrival (vertical magenta line in Figure 2). During this time segment, MAVEN traveled outbound away from periaapsis in the nightside magnetosheath region (Figure 3a). The ambient magnetic field strength observed by the magnetometer (MAG) [Connerney *et al.*, 2015] was ~ 20 nT on average during the entire time period (Figure 3g). MAG detected two consecutive steep magnetic field enhancements, reaching a peak strength of ~ 80 nT at the times marked by magenta and light blue horizontal bars in Figure 3g. We hereafter refer to these events during magenta (light blue) bars as Events 1 (2). Both magnetic field enhancements were short duration, < 5 s. Hodograms of the magnetic field components in the minimum variance analysis (MVA) coordinate systems [e.g., Sonnerup and Scheible, 1998] for Event 1 (Figure 4a) clearly shows that the magnetic field vector rotates smoothly in the plane perpendicular to the minimum variance axis (B_k). Event 2 also has a similar hodogram pattern (shown as Figure S1 in the supporting information). The eigenvalue ratio of the intermediate to minimum variance axis for Events 1(2) is approximately 15.4(24.9) (i.e., $\lambda_j/\lambda_k \approx 15.4(24.9)$). Hence, both events can be described by magnetic flux ropes, because this feature seen in the hodograms corresponds to the typical flux rope signature [e.g., Russell and Elphic, 1979; Vignes *et al.*, 2004]. As shown in Figure 1, these observed flux ropes during the ICME passage have fields likely a few times stronger than those detected at comparably high altitudes (> 1000 km) under the relatively steady solar wind state [Hara *et al.*, 2015; DiBraccio *et al.*, 2015].

The Supra-Thermal And Thermal Ion Composition (STATIC) experiment can measure three-dimensional velocity distribution functions with ions while resolving their compositions [McFadden *et al.*, 2015]. Hence, STATIC can provide mass resolution of ion populations inside the observed flux ropes. Because the observed ion flux was at a higher intensity than usual owing to the ICME passage, some contamination constituents including stragglers, scattered and sputtered ions from the spacecraft and/or instrument itself [McFadden *et al.*, 2015] were also enhanced. In our analysis, we removed these stragglers at least from the lowest mass populations, which had the highest contribution of background. Figure 3d was shown after subtracting their stragglers. STATIC measurements (Figures 3b–3d) indicate steep ion composition changes across both structures: the solar wind (magnetosheath) origin low-mass (protons and alphas) ions were decreased in both energy and flux, while planetary origin high-mass (O^+ and O_2^+) ion were increased. This feature is similar to Hara *et al.* [2015], meanwhile, the observed energy range was higher than a few keV (Figure 3c). This energy range of planetary ions is thus higher than that of ambient solar wind ions. Moreover, in particular, for Event 1, STATIC also measured planetary ions with energies less than 10 eV. However, the STATIC ion angular distribution (not shown here) confirmed that such low-energy planetary ions were mostly coming from the spacecraft. Therefore, these low-energy ions may be more accurately interpreted as background populations caused by the intense high-energy planetary ions across the structure.

Solar Wind Ion Analyzer (SWIA) can also sample the ion energy and angular distribution every 4 s without compositions. The lowest energy is ~ 25 eV during this period [Halekas *et al.*, 2015]. As shown in Figure 3e, SWIA also recorded ion populations with energies both higher than a few keV and less than a few tens of eV across both structures. This tendency is similar to the STATIC observations. It should also be noted that these low-energy ions are detected in SWIA angular bins, which are generally blocked by the spacecraft itself. Hence, such low-energy ion populations also tend to be caused by enhancements of high-energy ion populations across these structures. The observed timing of low-energy ions is slightly different between STATIC and SWIA (Figures 3c and 3e), because the fields of view (FOV) are not completely coincident. To summarize the ion behaviors recorded by STATIC and SWIA during the events: planetary heavy ions higher than a few keV are (mostly) enhanced across the flux ropes.

The electrons' energy and angular spectra, as well as their pitch angle distributions (PADs) relative to the local magnetic field direction, can be obtained from Solar Wind Electron Analyzer (SWEA) [Mitchell *et al.*, 2016]. Figure 3f indicates that variations of the energy spectra for electrons tend to be coincident with those of the ion compositions across these structures. Namely, the observed electrons with energies higher than about

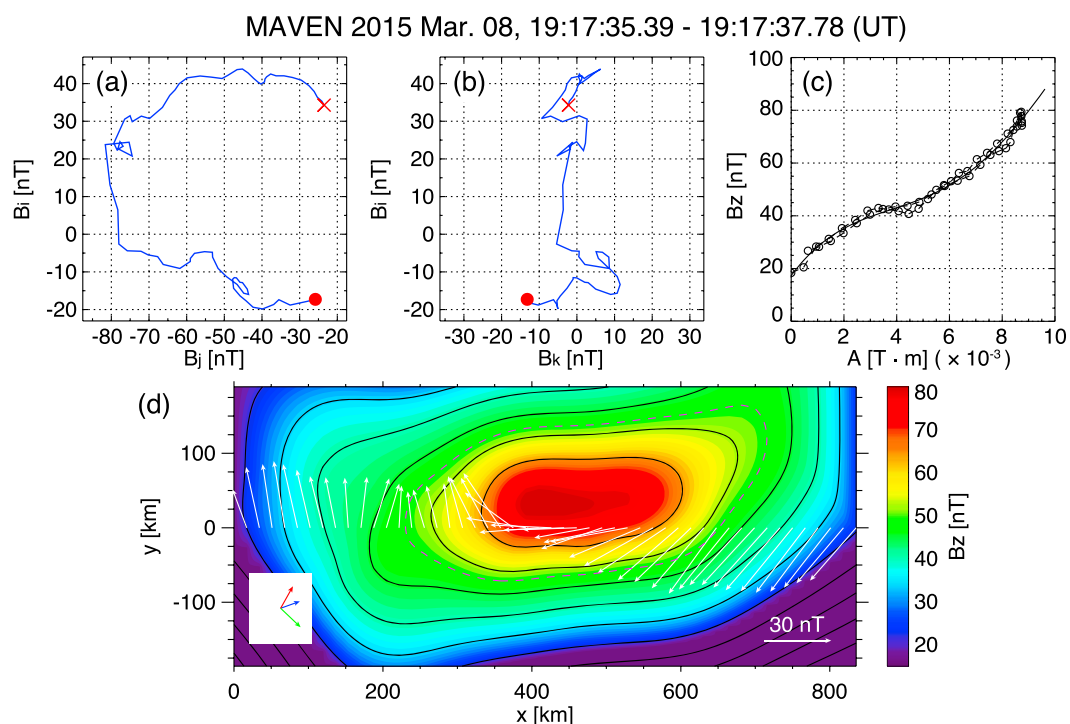


Figure 4. Overview of the flux rope spatial properties for Event 1: (a, b) The hodograms of magnetic field components in the minimum variance analysis (MVA) coordinate system, where B_i , B_j , and B_k components refer to the maximum, intermediate, and minimum variance axes, respectively. Red circles (crosses) are start (end) points. (c) The axial magnetic field B_z plotted as a function of the vector potential A . Open circles are MAVEN observations and the solid curve denotes the fitted polynomials. (d) The two-dimensional axial magnetic field B_z map recovered from the Grad-Shafranov reconstruction technique based on the MAVEN observations. MAVEN traversed (time progressed) from left to right along $y = 0$. White arrows represent the transverse measured magnetic field components. The colored arrows shown at the lower left corner on the reconstructed map are the projections of MSO unit vectors, X_{mso} (blue), Y_{mso} (green), and Z_{mso} (red), respectively. Overlaid dashed magenta curve is the boundary to estimate the flux rope volume. The method to define this boundary is given in text.

100 eV are enhanced in Event 1, while electrons with energies of several tens of eV are enhanced in Event 2. Note that the PAD data is available every 4 s at this interval [Mitchell *et al.*, 2016]; therefore, it would be difficult to deduce further clues associated with magnetic topologies of the flux rope from the PAD data.

4. Estimation of Flux Ropes' Spatial Properties Reconstructed via the Grad-Shafranov Equation

To roughly estimate the spatial properties of the observed flux ropes, we apply the Grad-Shafranov reconstruction (GSR) technique, which is capable of recovering magnetohydrostatic structures like the observed flux ropes, using the single-spacecraft in situ measurements. The assumptions to apply this technique are that the structure is two dimensional and time independent [e.g., Sturrock, 1994; Sonnerup and Guo, 1996]. The GSR technique has been used for more than two decades to recover various magnetohydrostatic structures seen in space plasma, such as flux ropes observed in interplanetary space (often known as magnetic clouds) [e.g., Hau and Sonnerup, 1999; Hu and Sonnerup, 2002] and observed in Earth's magnetosphere (often called flux transfer events) [e.g., Sonnerup *et al.*, 2004; Hasegawa *et al.*, 2006].

Hara *et al.* [2014a, 2014b] previously investigated the magnetic flux ropes observed by MGS around Mars to understand the possible ion escape rates associated with flux ropes, although MGS lacked the ion measurements. Recently, Hara *et al.* [2015] recovered the spatial structure of a detached magnetic flux rope based on the MAVEN simultaneous plasma and magnetic field measurements. The basic procedure to apply the GSR technique is similar to previous studies [e.g., Hau and Sonnerup, 1999; Hu and Sonnerup, 2001, 2002; Hasegawa *et al.*, 2012], with the specific treatments optimized to apply the GSR technique to the Martian flux ropes detected by MAVEN extensively described in Hara *et al.* [2015].

It should be noted here that we find difficulties uniquely reconstructing the spatial structure for Event 2, perhaps because part of the assumptions adopted to apply the GSR technique might be invalid (e.g., the observed structure evolves in time, and/or it is not two dimensional but three dimensional). The GSR prediction for Event 2 also implies that MAVEN was a remote encounter with Event 2, i.e., traversed far from the center of the flux rope. As a consequence, we only investigate the detailed flux rope spatial properties for Event 1.

STATIC ion measurements are used in the GSR technique as the plasma data. However, as mentioned in section 3, the duration across the structure was as short as only <5 s. On the other hand, the STATIC data are available as fast as every 4 s [McFadden *et al.*, 2015]. Taking into account the observational limitations, the plasma data subsets used as input to the GSR technique are as follows: The ion density-weighted bulk velocity is computed from the STATIC three-dimensional distribution functions (16 s cadences) under the assumption that all the ion species are comoving with a flux rope, and a simple spline interpolation is performed over the time period across the structure; a constant plasma pressure is given because a single STATIC measurement is only available across the structure. It means that we assume a force-free ($\nabla p = 0$) approximation.

In a basic procedure to apply the GSR technique, the deHoffmann-Teller (HT) frame transformation is necessary, because the HT velocity, \mathbf{V}_{HT} , allows for the time series data to be converted into the spatial information at points along the spacecraft path [e.g., *Hau and Sonnerup*, 1999; *Hu and Sonnerup*, 2002; *Hasegawa et al.*, 2012; *Hara et al.*, 2015]. The HT velocity, \mathbf{V}_{HT} , is found to be $[-527.0 \ -89.8, \ 79.8]$ km/s in the MSO coordinates. This estimated velocity is at least an order of magnitude faster than that of a typical detached flux rope reported in *Hara et al.* [2015]. The correction coefficient for the HT analysis is quite high ($cc = 0.99985$), which is well satisfied with a magnetohydrostatic structure. The Walén slope for the GSR interval is so small (0.026) that this event turns out to be suitable for applying the GSR technique. Figure 4d shows the reconstructed axial field map of Event 1. The correlation of the magnetic field components between the MAVEN measurements and the GSR prediction is also quite high ($cc = 0.99941$), indicating that the spatial structure is well reconstructed by the GSR technique. Figure 4c displays that the observed data points can be fitted by single polynomial curve (black solid curve), suggesting that it is a reasonable assumption that the structure was under two dimensional. The axial orientation is estimated to be $[0.761, \ -0.357, \ -0.541]$ in the MSO coordinates. The dashed magenta curve onto Figure 4d is the boundary defined as a surface where the reconstructed axial field strength is 50% of the core field value. The equivalent radius is ~ 161.7 km computed from the cross section of the reconstructed map, under the assumption that the flux rope shape is strictly circular. The rope length along the flux rope axis is ~ 482.6 km, estimated from the MAVEN flight distance in the HT frame, assuming that the structure is maintained at least over the time when MAVEN traversed the flux rope. *Harnett* [2009] performed three-dimensional multifluid simulations of the Martian induced magnetosphere in order to understand the development and dynamics of flux ropes. The estimated flux rope spatial scale is smaller than her simulation predictions [*Harnett*, 2009]. On the other hand, these spatial properties are comparable to the previous event reported in *Hara et al.* [2015]. However, the core axial field strength of this event is a few times stronger than that seen in the case from the relative steady solar wind period.

5. Summary and Discussions of Possible ICME Effects

In this paper, we presented two magnetic flux ropes with a strong axial field observed by MAVEN during the 8 March 2015 ICME event. These events were observed in the nightside flank magnetosheath region and observed altitude is as high as >5000 km. The observed durations were shorter than 5 s, and the magnetic field reached a peak strength of >80 nT (Figure 3g). These observed fields are a few times stronger than those seen in the similar location under relative steady solar wind states [*Hara et al.*, 2015]. Hence, these are the first unique observations that MAVEN detected such flux ropes with a strong field at high altitudes (Figure 1). These results suggest that the strong IMF amplitude and dynamic pressure due to the ICME passage were responsible for creating such observed, more extreme flux ropes.

We succeeded in uniquely recovering the spatial structure and axial orientation of the observed flux rope for Event 1 by using the Grad-Shafranov reconstruction (GSR) technique. The GSR results indicate that the estimated spatial scales described in section 4 are comparable to the detached event recently reported in *Hara et al.* [2015] and those seen downstream from the strong crustal fields as detected on MGS [*Hara et al.*, 2014a, 2014b].

At that time of crossing these structures, STATIC simultaneously detected planetary heavy ions with energies of higher than a few keV (Figures 3c and 3d). This result indicates that these flux ropes likely formed in the

vicinity of the Martian ionosphere. Moreover, since the observed altitude was higher than 5000 km, quite far from the main Martian ionosphere, one interpretation is that these flux ropes detached from the main ionosphere and were in the process of moving outward into interplanetary space.

Here we noted some comments for this interpretation. First, the bulk flow should be the same regardless of ion species. STATIC three-dimensional velocity distributions indicate that the bulk flow is roughly a comparable speed regardless of the ion species and is moving approximately along the convection direction. This feature can be consistent with our interpretation that all the ion species are comoving with this structure. Second, comparing the spatial scale of the flux rope estimated by GSR with the gyroradii of the observed planetary ions with energies larger than a few keV, their gyroradii are larger than the rope spatial scale in an inertial frame of reference. However, viewing from the comoving frame with the structure, their gyroradii can be small sufficient to trap inside the flux ropes. It is likely that a fraction of the planetary ions initially trapped inside the flux rope have already been lost presumably into space. On the other hand, we might be able to alternatively interpret that the possible source of high-energy populations is merely owing to pickup planetary heavy ions. However, we are unable find high-energy populations around the structure. Assuming that the global behaviors of pickup ions can be determined by the upstream motional electric field, this event was observed in the $-\mathbf{E}$ hemisphere, because the spacecraft was in the dawn sector, and the magnetic field direction is stably oriented along $-B_z$ around the structure (see, Figure 3h). Hence, this configuration is unfavorable to measure the high-energy pickup heavy ions like “polar plume” [Y. Dong *et al.*, 2015].

One remarkable feature associated with the ICME effects is that the estimated flux rope speed is at least an order of magnitude faster than a detached flux rope event recently measured under a relative steady solar wind state [Hara *et al.*, 2015]. This estimated velocity is more than sufficiently high to be able to escape from Mars. Given that the nominal planetary ion populations are initially trapped inside the structure, the possible ion escape rates through the flux rope might also increase owing to the ICME passage, assuming that associated planetary ions are completely removed during the MAVEN’s traversal of the structure. Our plans are to continue to analyze flux ropes observed by MAVEN, including their planetary ion associations and dependence on external (and crustal field orientation) conditions, toward a better understanding of the roles played by these structures in the Mars solar wind interaction-related ion escape.

Acknowledgments

The MAVEN data used in this paper are publicly available in NASA’s Planetary Data System (<http://ppi.pds.nasa.gov/mission/MAVEN>). Analysis of SWEA data was partially supported by CNES. This work was carried out by the joint research programs of the Solar-Terrestrial Environment Laboratory (currently, Institute for Space-Earth Environmental Research), Nagoya University. T. Hara thanks C. O. Lee for helpful discussions with respect to the ICME events observed by MAVEN. G. A. DiBraccio was supported by a NASA Postdoctoral Program appointment at the NASA Goddard Space Flight Center, administered by Oak Ridge Associated Universities through a contract with NASA.

References

- Acuña, M. H., et al. (1998), Magnetic field and plasma observations at Mars: Initial results of the Mars Global Surveyor mission, *Science*, 279, 1676–1680, doi:10.1126/science.279.5357.1676.
- Acuña, M. H., et al. (1999), Global distribution of crustal magnetization discovered by the Mars Global Surveyor MAG/ER experiment, *Science*, 284, 790–793, doi:10.1126/science.284.5415.790.
- Barabash, S., A. Fedorov, R. Lundin, and J.-A. Sauvaud (2007), Martian atmospheric erosion rates, *Science*, 315, 501–503, doi:10.1126/science.1134358.
- Beharrell, M. J., and J. A. Wild (2012), Stationary flux ropes at the southern terminator of Mars, *J. Geophys. Res.*, 117, A12212, doi:10.1029/2012JA017738.
- Brain, D. A., A. H. Baker, J. Briggs, J. P. Eastwood, J. S. Halekas, and T.-D. Phan (2010), Episodic detachment of Martian crustal magnetic fields leading to bulk atmospheric plasma escape, *Geophys. Res. Lett.*, 37, L14108, doi:10.1029/2010GL043916.
- Brain, D. A., et al. (2015), The spatial distribution of planetary ion fluxes near Mars observed by MAVEN, *Geophys. Res. Lett.*, 42, 9142–9148, doi:10.1002/2015GL065293.
- Briggs, J. A., D. A. Brain, M. L. Cartwright, J. P. Eastwood, and J. S. Halekas (2011), A statistical study of flux ropes in the Martian magnetosphere, *Planet. Space Sci.*, 59, 1498–1505, doi:10.1016/j.pss.2011.06.010.
- Cloutier, P. A., et al. (1999), Venus-like interaction of the solar wind with Mars, *Geophys. Res. Lett.*, 26(17), 2685–2688, doi:10.1029/1999GL900591.
- Connerney, J. E. P., J. Espley, P. Lawton, S. Murphy, J. Odum, R. Oliverson, and D. Sheppard (2015), The MAVEN magnetic field investigation, *Space Sci. Rev.*, 195, 257–291, doi:10.1007/s11214-015-0169-4.
- Curry, S. M., et al. (2015), Response of Mars O⁺ pickup ions to the 8 March 2015 ICME: Inferences from MAVEN data-based models, *Geophys. Res. Lett.*, 42, 9095–9102, doi:10.1002/2015GL065304.
- DiBraccio, G. A., et al. (2015), Magnetotail dynamics at Mars: Initial MAVEN observations, *Geophys. Res. Lett.*, 42, 8828–8837, doi:10.1002/2015GL065248.
- Dong, C. F., et al. (2015), Multifluid MHD study of the solar wind interaction with Mars’ upper atmosphere during the 2015 March 8th ICME event, *Geophys. Res. Lett.*, 42, 9103–9112, doi:10.1002/2015GL065944.
- Dong, Y., X. Fang, D. A. Brain, J. P. McFadden, J. S. Halekas, J. E. Connerney, S. M. Curry, Y. Harada, J. G. Luhmann, and B. M. Jakosky (2015), Strong plume fluxes at Mars observed by MAVEN: An important planetary ion escape channel, *Geophys. Res. Lett.*, 42, 8942–8950, doi:10.1002/2015GL065346.
- Dubinin, E., M. Fränz, J. Woch, F. Duru, D. Gurnett, R. Modolo, S. Barabash, and R. Lundin (2009), Ionospheric storms on Mars: Impact of the corotating interaction region, *Geophys. Res. Lett.*, 36, L01105, doi:10.1029/2008GL036559.
- Edberg, N. J. T., H. Nilsson, A. O. Williams, M. Lester, S. E. Milan, S. W. H. Cowley, M. Fränz, S. Barabash, and Y. Futaana (2010), Pumping out the atmosphere of Mars through solar wind pressure pulses, *Geophys. Res. Lett.*, 37, L03107, doi:10.1029/2009GL041814.
- Edberg, N. J. T., et al. (2011), Atmospheric erosion of Venus during stormy space weather, *J. Geophys. Res.*, 116, A09308, doi:10.1029/2011JA016749.

- Futaana, Y., et al. (2008), Mars Express and Venus Express multi-point observations of geoeffective solar flare events in December 2006, *Planet. Space Sci.*, *56*, 873–880, doi:10.1016/j.pss.2007.10.014.
- Halekas, J. S., E. R. Taylor, G. Dalton, G. Johnson, D. W. Curtis, J. P. McFadden, D. L. Mitchell, R. P. Lin, and B. M. Jakosky (2015), The solar wind ion analyzer for MAVEN, *Space Sci. Rev.*, *195*, 125–151, doi:10.1007/s11214-013-0029-z.
- Hara, T., K. Seki, H. Hasegawa, D. A. Brain, K. Matsunaga, and M. H. Saito (2014a), The spatial structure of Martian magnetic flux ropes recovered by the Grad-Shafranov reconstruction technique, *J. Geophys. Res. Space Physics*, *119*, 1262–1271, doi:10.1002/2013JA019414.
- Hara, T., K. Seki, H. Hasegawa, D. A. Brain, K. Matsunaga, M. H. Saito, and D. Shiota (2014b), Formation processes of flux ropes downstream from Martian crustal magnetic fields inferred from Grad-Shafranov reconstruction, *J. Geophys. Res. Space Physics*, *119*, 7947–7962, doi:10.1002/2014JA019943.
- Hara, T., et al. (2015), Estimation of the spatial structure of a detached magnetic flux rope at Mars based on simultaneous MAVEN plasma and magnetic field observations, *Geophys. Res. Lett.*, *42*, 8933–8941, doi:10.1002/2015GL065720.
- Harnett, E. M. (2009), High-resolution multifluid simulations of flux ropes in the Martian magnetosphere, *J. Geophys. Res.*, *114*, A01208, doi:10.1029/2008JA013648.
- Hasegawa, H., B. U. Ö. Sonnerup, C. J. Owen, B. Klecker, G. Paschmann, A. Balogh, and H. Rème (2006), The structure of flux transfer events recovered from Cluster data, *Ann. Geophys.*, *24*, 603–618, doi:10.5194/angeo-24-603-2006.
- Hasegawa, H., H. Zhang, Y. Lin, B. U. Ö. Sonnerup, S. J. Schwartz, B. Lavraud, and Q.-G. Zong (2012), Magnetic flux rope formation within a magnetosheath hot flow anomaly, *J. Geophys. Res.*, *117*, A09214, doi:10.1029/2012JA017920.
- Hau, L.-N., and B. U. Ö. Sonnerup (1999), Two-dimensional coherent structures in the magnetopause: Recovery of static equilibria from single-spacecraft data, *J. Geophys. Res.*, *104*, 6899–6918, doi:10.1029/1999JA900002.
- Hu, Q., and B. U. Ö. Sonnerup (2001), Reconstruction of magnetic flux ropes in the solar wind, *Geophys. Res. Lett.*, *28*, 467–470, doi:10.1029/2000GL012232.
- Hu, Q., and B. U. Ö. Sonnerup (2002), Reconstruction of magnetic clouds in the solar wind: Orientations and configurations, *J. Geophys. Res.*, *107*(A7), 1142, doi:10.1029/2001JA000293.
- Jakosky, B. M., et al. (2015a), The Mars Atmosphere and Volatile Evolution (MAVEN) mission, *Space Sci. Rev.*, *195*, 3–48, doi:10.1007/s11214-015-0139-x.
- Jakosky, B. M., J. M. Grebowsky, J. G. Luhmann, and D. A. Brain (2015b), Initial results from the MAVEN mission to Mars, *Geophys. Res. Lett.*, *42*, 8791–8802, doi:10.1002/2015GL065271.
- Jakosky, B. M., et al. (2015c), MAVEN observations of the response of Mars to an interplanetary coronal mass ejection, *Science*, *350*(6261), aad0210, doi:10.1126/science.aad0210.
- Luhmann, J. G., W. T. Kasprzak, and C. T. Russell (2007), Space weather at Venus and its potential consequences for atmosphere evolution, *J. Geophys. Res.*, *112*, E04510, doi:10.1029/2006JE002820.
- Luhmann, J. G., A. Fedorov, S. Barabash, E. Carlsson, Y. Futaana, T. L. Zhang, C. T. Russell, J. G. Lyon, S. A. Ledvina, and D. A. Brain (2008), Venus Express observations of atmospheric oxygen escape during the passage of several coronal mass ejections, *J. Geophys. Res.*, *113*, E00B04, doi:10.1029/2008JE003092.
- Lundin, R. (2011), Ion acceleration and outflow from Mars and Venus: An overview, *Space Sci. Rev.*, *162*, 309–334, doi:10.1007/s11214-011-9811-y.
- Lundin, R., H. Borg, B. Hultqvist, A. Zakharov, and R. Pellinen (1989), First measurements of the ionospheric plasma escape from Mars, *Nature*, *341*, 609–612, doi:10.1038/341609a0.
- Lundin, R., S. Barabash, A. Fedorov, M. Holmström, H. Nilsson, J.-A. Sauvaud, and M. Yamauchi (2008), Solar forcing and planetary ion escape from Mars, *Geophys. Res. Lett.*, *35*, L09203, doi:10.1029/2007GL032884.
- Lundin, R., S. Barabash, M. Holmström, H. Nilsson, Y. Futaana, R. Ramstad, M. Yamauchi, E. Dubinin, and M. Fraenz (2013), Solar cycle effects on the ion escape from Mars, *Geophys. Res. Lett.*, *40*, 6028–6032, doi:10.1002/2013GL058154.
- McFadden, J. P., et al. (2015), MAVEN SupraThermal and Thermal Ion Composition (STATIC) instrument, *Space Sci. Rev.*, *195*, 199–256, doi:10.1007/s11214-015-0175-6.
- Mitchell, D. L., et al. (2016), The MAVEN solar wind electron analyzer, *Space Sci. Rev.*, *200*, 495–528, doi:10.1007/s11214-015-0232-1.
- Morgan, D. D., D. A. Gurnett, F. Akalin, D. A. Brain, J. S. Leisner, F. Duru, R. A. Frahm, and J. D. Wittingham (2011), Dual-spacecraft observation of large-scale magnetic flux ropes in the Martian ionosphere, *J. Geophys. Res.*, *116*, A02319, doi:10.1029/2010JA016134.
- Morgan, D. D., et al. (2014), Effects of a strong ICME on the Martian ionosphere as detected by Mars Express and Mars Odyssey, *J. Geophys. Res. Space Physics*, *119*, 5891–5908, doi:10.1002/2013JA019522.
- Morschhauser, A., V. Lesur, and M. Grott (2014), A spherical harmonic model of the lithospheric magnetic field of Mars, *J. Geophys. Res. Planets*, *119*, 1162–1188, doi:10.1002/2013JE004555.
- Nilsson, H., E. Carlsson, D. A. Brain, M. Yamauchi, M. Holmström, S. Barabash, R. Lundin, and Y. Futaana (2010), Ion escape from Mars as a function of solar wind conditions: A statistical study, *Icarus*, *40*–49, doi:10.1016/j.icarus.2009.03.006.
- Opgenoorth, H. J., D. J. Andrews, M. Fränz, M. Lester, N. J. T. Edberg, D. Morgan, F. Duru, O. Witasse, and A. O. Williams (2013), Mars ionospheric response to solar wind variability, *J. Geophys. Res. Space Physics*, *118*, 6558–6587, doi:10.1002/jgra.50537.
- Russell, C. T., and R. C. Elphic (1979), Observation of magnetic flux ropes in the Venus ionosphere, *Nature*, *279*, 616–618, doi:10.1038/279616a0.
- Schneider, N. M., et al. (2015), Discovery of diffuse aurora on Mars, *Science*, *350*(6261), aad0313, doi:10.1126/science.aad0313.
- Sonnerup, B. U. Ö., and M. Guo (1996), Magnetopause transects, *Geophys. Res. Lett.*, *23*, 3679–3682, doi:10.1029/96GL03573.
- Sonnerup, B. U. Ö., and M. Scheible (1998), Minimum and maximum variance analysis, in *Analysis Methods for Multi-Spacecraft Data*, ISSI Sci. Rep. Ser., vol. 1, edited by G. Paschmann and P. Daly, pp. 185–220, Eur. Space Agency, Paris.
- Sonnerup, B. U. Ö., H. Hasegawa, and G. Paschmann (2004), Anatomy of a flux transfer event seen by Cluster, *Geophys. Res. Lett.*, *31*, L11803, doi:10.1029/2004GL020134.
- Sturrock, P. A. (1994), *Plasma Physics: An Introduction to the Theory of Astrophysical, Geophysical and Laboratory Plasmas*, Stanford-Cambridge Program, Cambridge Univ. Press, Cambridge, U. K.
- Trotignon, J. G., C. Mazelle, C. Bertucci, and M. H. Acuña (2006), Martian shock and magnetic pile-up boundary positions and shapes determined from the Phobos 2 and Mars Global Surveyor data sets, *Planet. Space Sci.*, *54*, 357–369, doi:10.1016/j.pss.2006.01.003.
- Vignes, D., M. H. Acuña, J. E. P. Connerney, D. H. Crider, H. Rème, and C. Mazelle (2004), Magnetic flux ropes in the Martian atmosphere: Global characteristics, *Space Sci. Rev.*, *111*, 223–231, doi:10.1023/B:SPAC.0000032716.21619.f2.